Single and multi-component adsorption of psychiatric pharmaceuticals onto alternative and commercial carbons

Vânia Calisto[a*], *Guilaine Jaria*[a], *Carla Patrícia Silva*[a], *Catarina I. A. Ferreira*[a], *Marta Otero*[b], *Valdemar I. Esteves*[a]

[a] Department of Chemistry and CESAM (Centre for Environmental and Marine Studies), University of Aveiro, Campus de Santiago, 3810-193 Aveiro, Portugal

[b] Department of Applied Chemistry and Physics, IMARENABIO, University of Léon, Campus de Vegazana, Léon, Spain

[*]Corresponding author: Tel.: +351 234401408; E-mail address: vania.calisto@ua.pt

Abstract

This work describes the adsorptive removal of three widely consumed psychiatric pharmaceuticals (carbamazepine, paroxetine and oxazepam) from ultrapure water. Two different adsorbents were used: a commercial activated carbon and a non-activated waste-based carbon (PS800-150-HCl), produced by pyrolysis of primary paper mill sludge. These adsorbents were used in single, binary and ternary batch experiments in order to determine the adsorption kinetics and equilibrium isotherms of the considered pharmaceuticals. For the three drugs and both carbons, the equilibrium was quickly attained (with maximum equilibrium times of 15 and 120 min for the waste-based and the commercial carbons, respectively) even in binary and ternary systems. Single component equilibrium data were adequately described by the Langmuir model, with the commercial carbon registering higher maximum adsorption capacities (between 272 ± 10 and 493 ± 12 μmol g^{-1}) than PS800-150-HCl (between 64 ± 2 and 74 ± 1 μmol g^{-1}). Multi-component equilibrium data were also best fitted by the single component Langmuir isotherm, followed by the Langmuir competitive model. Overall, competitive effects did not largely affect the performance of both adsorbents. Binary and ternary systems maintained fast kinetics, the individual maximum adsorption capacities were not lower than half of the single component systems and both carbons presented improved total adsorption capacities for multi-component solutions.

Keywords: Environment; Water Treatment; Paper mill sludge; Remediation; Emerging contaminants

1. Introduction

The global occurrence of pharmaceuticals in the environment is now a reasonably well-documented reality. The number of studies reporting their presence in surface, ground and even drinking waters has grown exponentially in the last few years (Alygizakis et al., 2016; Calisto and Esteves, 2009; Daughton and Ternes, 1999; Li, 2014; Loos et al., 2010; Luo et al., 2014), constituting a first indication that the water resources quality is actually being affected. The environmental pressure exerted by these contaminants is expected to raise in the next decades, mainly due to the worldwide ageing of the population, high prevalence of chronic diseases and easy accessibility of medical care (OECD, 2015). Within this scenario, and in order to mitigate the environmental contamination by pharmaceuticals, the main sources of discharges of these pollutants into the environment should be effectively addressed. In fact, the European Union has already recognized the urgency of solving water pollution by pharmaceuticals by evaluating new ways of reducing their input into environmental matrices, taking into consideration public health and cost-effectiveness, according to the Directive 2013/39 EU (European Parliament, 2013). Waste Water Treatment Plants (WWTPs) were projected to reduce pollutants according with legislated parameters but not to eliminate pharmaceuticals. In fact, there is a large number of studies reporting that the treatments applied in conventional WWTPs are not adequate to remove these pollutants (Bahlmann et al., 2014; Calisto et al., 2011a; Margot et al., 2013). As a result, the discharge of contaminated effluents from these facilities (both urban and industrial) is the primary pathway of pharmaceuticals into the environment (Alygizakis et al., 2016; Cardoso et al., 2014; Jelic et al., 2011). Thus, developing effective methodologies to be applied as WWTPs tertiary treatment might be a feasible path for the minimization of the environmental impact of pharmaceuticals.

In this context, amongst the several advanced treatments proposed in the literature, adsorption is considered to be an interesting option due its versatility, efficiency, non-generation of transformation by-products and easiness of implementation when compared with other advanced treatments (Gupta and Saleh, 2013; Margot et al., 2013; Nam et al., 2014; Yu et al., 2009). However, the most commonly applied adsorbents, activated carbons, are in general

expensive and have with high regeneration costs. These drawbacks have motivated the search for alternative adsorbents, including materials produced from agricultural and industrial wastes (Bhatnagar and Sillanpää, 2010; Calisto et al., 2015; Fernandez et al., 2015; Ferreira et al., 2015; Ioannidou and Zabaniotou, 2007; Mohan et al., 2014). Such an option also constitutes a new route for the management and economic valorization of these residues, simultaneously offering starting materials at low or no cost, which is the main concept behind circular economy (European Comission, 2014).

The study of the application of alternative adsorbents for the removal of pharmaceuticals from water is scarcely addressed in the literature (specially, in comparison with the huge number of studies concerning inorganic pollutants or other organic pollutants such as textile dyes or pesticides). Additionally, to our best knowledge, there are only a few studies on the adsorption of pharmaceuticals in multi-solute systems (Jung et al., 2015; Mansouri et al., 2015; Nielsen and Bandosz, 2016; Sotelo et al., 2014), all considering ultra-pure water as the background matrix. In fact, most of studies focus on the single adsorption of drugs so obviating multi-solute competitive effects occurring in real systems, where the performance of the adsorbent might be significantly modified due to possible competition of the different adsorbates for the vacant adsorption sites (Limousin et al., 2007). Accordingly, multi-component adsorption data are essential for the design of treatment systems (Noroozi and Sorial, 2013) and, thus, the scarcity of such data was the main motivation for the work here presented. This manuscript describes the single, binary and ternary adsorptive removal of three widely consumed psychiatric pharmaceuticals (carbamazepine, oxazepam and paroxetine) from ultrapure water, by a commercial activated carbon and an alternative waste-based carbon produced by pyrolysis of primary paper mill sludge with the aim of evaluating and comparing the performance of the studied carbons under competitive effects.

2. Experimental section

2.1 Pharmaceuticals

Adsorption studies were performed with three pharmaceuticals: the antiepileptic carbamazepine (CBZ), Sigma Aldrich, 99%; the anxiolytic oxazepam (OXZ), TCI Europe, >98%; the antidepressant paroxetine (PAR), TCI Europe, >98%. Physico-chemical properties of these pharmaceuticals are summarized in Supplementary Material (SM), Table S1.

2.2 Adsorbents

Two powdered carbons were used as adsorbents for the removal of the pharmaceuticals from water: a commercially available activated carbon (PBFG4, provided by ChemViron Carbon) and an alternative waste-based non-activated carbon (PS800-150-HCl). PS800-150-HCl was produced by the pyrolysis of paper mill sludge, under nitrogen controlled atmosphere at 800 ºC, with a residence time of 150 min. Detailed information concerning the pyrolysis process and the selection of the production conditions can be found in a previous work (Calisto et al., 2014). After pyrolysis, the carbon was washed with 1.2 M HCl followed by distilled water until the washing solution reaching neutral pH. The washing procedure was aimed at removing ashes and other inorganic matter, improving the microporosity and the surface area of the material by unblocking obstructed pores. Finally, the carbon was oven dried at 105 ºC for 24h.

2.2.1 Characterization of the adsorbents

PBFG4 and PS800-150-HCl were characterized by means of elemental analyses, total and inorganic carbon analysis, point of zero charge (PZC) and N_2 adsorption isotherms for the determination of surface area and microporosity. Detailed information concerning these procedures is given in SM.

2.3 Adsorption experiments - single, binary and ternary systems

Adsorption studies were performed using the batch experimental approach, in ultrapure water. Single (OXZ, PAR and CBZ), binary (CBZ+PAR, CBZ+OXZ and OXZ+PAR) and ternary (CBZ+PAR+OXZ) systems were studied, with each pharmaceutical at an initial concentration of 20 μmol L^{-1}. For this purpose, the pharmaceuticals solutions were put in contact with PBFG4 or PS800-150-HCl in polypropylene tubes and were shaken in a head-over-head shaker (Heidolph, Reax 2) at 50 rpm, under controlled temperature (25 ± 1ºC). Control experiments, consisting of the pharmaceutical(s) in the absence of the adsorbent, were run in parallel. All the experiments were performed in triplicate. After shaking, the samples were filtered through 0.22 μm PVDF filters (Millex, Millipore), after checking that the target compounds did not adsorb onto the referred filters, and analyzed for the concentration of the considered pharmaceuticals according to the procedure described in section 2.4. Then, the amount of the target pharmaceutical adsorbed onto the corresponding adsorbent q (μmol g^{-1}), was calculated by a mass balance relationship:

$$q = (C_0 - C)\frac{V}{m} \quad (1)$$

where C_0 (μmol L^{-1}) is the initial concentration of pharmaceutical, C is the pharmaceutical concentration after shaking (μmol L^{-1}), V is the volume of the solution (L) and m is the mass (g) of the corresponding adsorbent.

2.3.1 Adsorption kinetics

The time needed for each system to attain the adsorption equilibrium was determined by shaking single, binary and ternary pharmaceutical solutions with the corresponding adsorbent for different time intervals (between 5 and 240 min). The adsorbent concentration in kinetic experiments was 0.15 g L^{-1} for PS800-150-HCl and 0.025 g L^{-1} for PBFG4.

After shaking, the concentration of pharmaceuticals remaining in the aqueous phase for each time interval was determined and the amount of pharmaceutical adsorbed by mass unit of adsorbent at that time (q_t, μmol g^{-1}) was calculated by equation 1. The experimental data were

fitted to a pseudo-first and pseudo-second order kinetic models according to equations 2 (Lagergren, 1898) and 3 (Ho and McKay, 1999), respectively.

2) $q_t = q_e(1 - e^{-k_1 t})$

3) $q_t = \frac{q_e^2 k_2 t}{1 + q_e k_2 t}$

with t (min) representing the adsorbent/solution contact time, q_t (µmol g^{-1}) the amount of pharmaceutical adsorbed by mass unit of adsorbent at time t, q_e the amount of pharmaceutical adsorbed when the equilibrium is attained (µmol g^{-1}); and k_1 (min^{-1}) and k_2 (g µmol^{-1} min^{-1}) the pseudo-first and pseudo-second order rate constant, respectively. The mathematical modelling was performed using GraphPad Prism 5.

2.3.2 Adsorption equilibrium

Equilibrium adsorption experiments were performed by shaking single, binary or ternary solutions of pharmaceuticals with several adsorbent concentrations (ranging from 0.10 to 0.50 g L^{-1} for PS800-150-HCl and from 0.020 to 0.090 g L^{-1} for PBFG4) for the time needed to attain the equilibrium, as determined in section 2.3.1. Subsequently, the concentration of pharmaceutical(s) in the aqueous phase was determined, the amount of pharmaceutical adsorbed at equilibrium (q_e, µmol g^{-1}) calculated by the equation 1 and the experimental data fitted to non-linear models commonly used to describe the adsorption equilibrium isotherms. In a first approach, two single component isotherm models were applied to all systems: the Freundlich (Freundlich, 1906) and the Langmuir (Langmuir, 1918) models, represented by equations 4 and 5, respectively:

4) $q_e = K_F C_e^{1/N}$

5) $q_e = \frac{q_m K_L C_e}{1 + K_L C_e}$

with q_e representing the amount of solute adsorbed at equilibrium (µmol g^{-1}), C_e the amount of solute in the aqueous phase at equilibrium (µmol L^{-1}), K_F the Freundlich adsorption constant (µmol g-^{1} (µmol L^{-1})$^{-N}$), N the degree of non-linearity, q_m the maximum adsorption capacity

(μmol g^{-1}) and K_L (L μmol $^{-1}$) the Langmuir affinity coefficient. Modelling of the single and multi-component experimental data was performed using GraphPad Prism 5.

Additionally, fittings of equilibrium binary experimental data to multi-component isotherm models were determined. The following models were considered: competitive Langmuir model; non-competitive Langmuir model; and partially competitive Langmuir model (Kumar et al., 2008), as represented by equations 6 to 8, respectively. The presented equations are valid for a bi-component system, where *i* and *j* denotes parameters related with the species *i* and *j* of the binary system:

6) $$q_{e,i} = \frac{q_{m,i} K_{L,i} C_{e,i}}{1 + K_{L,i} C_{e,i} + K_{L,j} C_{e,j}}$$

where K_{Li} and K_{Lj} (L μmol $^{-1}$) are the Langmuir affinity coefficients;

7) $$q_{e,i} = \frac{q_{m,i} K_{L,i} C_{e,i} + b C_{e,i} C_{e,j}}{1 + K_{L,i} C_{e,i} + K_{L,j} C_{e,j} + b C_{e,i} C_{e,j}}$$

where all the parameters are defined as in equations 5 and 6, with the exception of *b* (L μmol $^{-1}$) which corresponds to an affinity adsorption constant related with the non-competitive adsorption;

8) $$q_{e,i} = \frac{q_{m,i} K_{L,i} C_{e,i} + K_{L,j} b_i C_{e,i} C_{e,j}}{1 + K_{L,i} C_{e,i} + K_{L,j} C_{e,j} + (K_{L,j} b_i + K_{L,j} b_j) C_{e,i} C_{e,j}}$$

where all the parameters are defined as in equations 5 and 6, with the exception of b_i and b_j (L μmol $^{-1}$) which correspond to adsorption constants of the affinity of the specie *i* for adsorption sites occupied by *j* and *vise-versa*, respectively.

The modelling of the bi-component experimental data to equations 6 to 8 was performed using the curve fitting toolbox of Matlab (version R2014a).

2.4 Micellar Electrokinetic Chromatography analyses

The quantification of CBZ, PAR and OXZ in aqueous solutions for the adsorption experiments was performed by Micellar Electrokinetic Chromatography (MECK) using a Beckman P/ACE MDQ instrument (Fullerton, CA, USA), equipped with a photodiode array detection system. For this purpose, a dynamically coated silica capillary with 40 cm (30 cm to

the detection window) was used, according to the procedure described in Calisto et al. (2011b) and here adapted for the simultaneous determination of the three studied pharmaceuticals. Briefly, the electrophoretic separation was performed at 25ºC, in direct polarity mode at 25 kV, during 5 min runs. Ethylvaniline was used as internal standard, spiked to all samples and standard solutions at a final concentration of 3.34 mg L^{-1}. Also, sodium tetraborate, at a final concentration of 10 mM, was added to all the samples and standard solutions, resulting in better peak shape, better resolution and enhanced repeatability. Detection was monitored at 200 nm for CBZ and PAR and at 214 for OXZ. Separation buffer consisted of 15 mM of sodium tetraborate and 30 mM of sodium dodecyl sulfate and was renewed every 6 runs. Capillary was washed between each run with ultrapure water for 1 min and separation buffer for 1.5 min at 20 psi. Additionally, capillary was washed with separation buffer, for 20 min, at the beginning of each working day in order to replenish the dynamic coating and with ultrapure water, for 10 min, at the end of the day. All the analyses were performed in triplicate. Calibration was performed by analyzing standard solutions with concentrations ranging from 1 to 20 µmol L^{-1}. Also, prior to the adsorption experiments, the adequacy of the optimized MEKC methodology to quantify the concentration of pharmaceuticals in the aqueous phase was tested by checking possible matrix effects.

3. Results and Discussion

3.1 Physico-chemical properties of the adsorbents

Table 1 summarizes the physico-chemical characterization of PBFG4, PS800-150-HCl and also primary sludge (the raw material used for the production of PS800-150-HCl). The commercial carbon PBFG4 has physical and chemical properties typical of an activated carbon, being mostly composed by carbon (81%, determined by elemental analysis) with a negligible percentage of inorganic carbon, and with a specific surface area of 848 m^2 g^{-1}. In turn, the produced carbon, PS800-150-HCl, has a lower carbon percentage (67%) and its surface area is 414 m^2 g^{-1}, which is approximately half of the one determined for PBFG4. However, one should note that PS800-150-HCl was not physically or chemically activated, having been produced by

the pyrolysis of paper mill sludge only followed by an acid washing step. On the other hand, as may be seen in Table 1, the PZC of the two carbons did not differ significantly.

3.2 Adsorption kinetics

The amount of each pharmaceutical adsorbed onto PS800-150-HCl or PBFG4 (q_t, µmol g^{-1}) *versus* contact time (t), for single and multicomponent solutions, is represented in Figure 1. The fitting parameters of the pseudo-first and pseudo-second order kinetic models to the experimental data are summarized in Table 2. In general, both pseudo-first and pseudo-second order kinetic models satisfactorily describe the experimental data for all the studied adsorbent-adsorbate(s) systems, with the large majority of the correlation coefficients above 0.97. Considering that the fitting of the pseudo-second order model presents the highest correlation coefficient for the largest number of systems, this discussion will be based on the kinetic parameters of this model; in addition, for clarity purposes, this is the only fitting represented in Figure 1 for each data set. The experimental data depicted in Figure 1 clearly show that the adsorption equilibrium of the studied pharmaceuticals onto PS800-150-HCl is quickly attained, with equilibrium times varying approximately from 5 to 15 minutes of contact time. On the other hand, the adsorption equilibrium onto PBFG4 is attained after 60 to 120 min. With respect to the three drugs here considered (in single systems), as for the k_2 shown in Table 2, the adsorption rate onto PS800-150-HCl is PAR>OXZ≈CBZ and onto PBFG4 it is OXZ>PAR≈CBZ.

Concerning the variation of the rate constant in the presence of possible competitors (Figure 2), one can conclude that, in the case of PS800-150-HCl, there are no significant differences for CBZ and OXZ. On the contrary, PAR is significantly affected in multi-component solutions, with a substantial decrease of the rate constant from single to binary systems (and both binary systems have similar k_2) and an additional decrease from the binary to the ternary systems. In relation to the adsorption onto PBFG4 (Figure 2), CBZ registered an increase of the adsorption rate constant from the single to multi-component solutions, with no statistical differences between binary and ternary systems. On the other hand, the adsorption

rate of PAR increases significantly from single and binary to ternary systems, while the adsorption rate of OXZ is not affected neither for binary nor for ternary solutions, similarly to the behavior observed for PS800-150-HCl.

Overall, PS800-150-HCl showed larger k_2 than PBFG4. Also, except for PAR onto PS800-150-HCl, no lower k_2 values were determined for the multi-component than for the single systems.

3.3 Adsorption equilibrium

3.3.1 Modelling of single-component isotherms to single and multi-component data

The adsorption isotherms of single and multi-component solutions, represented as the amount of the pharmaceutical adsorbed per mass unit of the adsorbent (q_e, μmol mg^{-1}) *versus* the equilibrium aqueous concentration of the pharmaceutical (C_e, μmol L^{-1}), are depicted in Figure 3. The fitting parameters to the isotherm models represented by equations 4 and 5 are summarized in Table 3. The 3-parameter Langmuir-Freundlich equilibrium model was also tested; the results were not considered in this discussion as it was the one that worst fitted the experimental data. According to R^2 and S_{yx} values in Table 3, the Langmuir model is the one that fits more adequately most of the adsorption isotherms onto PS800-150-HCl, while the Freundlich model is the one that best fits most of the adsorption isotherms onto PBFG4. However, considering that Langmuir fittings to PBFG4 experimental data are still very satisfactory, the Langmuir parameters will be selected for further discussion in order to allow a direct comparison of both carbons. In what concerns single component systems, and for both adsorbents, the Langmuir maximum adsorption capacities followed the order CBZ>OXZ>PAR, with the most adsorbed pharmaceuticals corresponding to the compounds with lower water solubility. However PBFG4 was the carbon with the highest adsorption capacities it also showed the most accentuated differences between the maximum adsorption capacities of the three pharmaceuticals, with q_m varying from 272 ± 10 μmol g^{-1} for PAR to 493 ± 12 μmol g^{-1} for CBZ. In opposition, PS800-150-HCl displayed very similar maximum adsorption capacities

for the three pharmaceuticals, varying only from 64 ± 2 μmol g^{-1} for PAR to 74 ± 1 μmol g^{-1} for CBZ. Regarding the Langmuir affinity coefficient, values obtained for the single isotherms onto PBFG4 were all lower than those onto PS800-150-HCl, which point to a higher affinity to the first.

A comparison between single and multi-component systems reveals that, in the case of PS800-150-HCl, the adsorption of CBZ and OXZ registered a decrease in the amount adsorbed (Figure 4). CBZ suffered the most accentuated difference from single to ternary systems, with a reduction in the amount adsorbed of approximately 50%. On the other hand, PAR was not negatively affected by the presence of the other two pharmaceuticals, with equivalent maximum adsorption capacities between single and binary systems and even slightly higher in ternary systems. The analysis of the Langmuir affinity constants shows that, besides the case of CBZ with no significant differences between systems, OXZ and PAR revealed a clear tendency to have lower K_L values in the multi-component solutions, meaning that the presence of possible competitors did not resulted in a reduced affinity of the pharmaceuticals to PS800-150-HCl. Concerning the adsorption onto PBFG4, the three pharmaceuticals registered a decrease in the maximum adsorption capacities for multi-component solutions (the most accentuated reduction is approximately 50%), with the exception of CBZ in the ternary system that is not significantly different from the result verified in the single solution (Figure 4). In relation to the Langmuir affinity constants, no significant differences were found for OXZ and PAR between single and multi-component adsorption, while CBZ showed a decrease in this parameter. Overall, similarly to PS800-150-HCl, the results did not point to a lower affinity (K_L) of the pharmaceuticals towards the adsorbent in the presence of possible competitors. Additionally, despite the observed reductions in the individual maximum adsorption capacities for multi-component systems, the analysis of the total maximum adsorption capacities for both adsorbents (Figure 5), revealed that the total amount of pharmaceutical(s) adsorbed by both carbons is consistently higher for binary and ternary mixtures than for single solutions. Nonetheless, the decrease of the individual adsorption capacities between single and multicomponent solutions is in agreement with other multi-component studies presented in the literature. Sotelo et al. (2014) reported a

decline of the maximum adsorption capacities of up to 30% in binary systems composed of diclofenac and caffeine, in comparison with the single adsorption of the same pharmaceuticals. More accentuated reductions were observed by Nielsen and Bandosz (2016), who registered a fall of up to 77% in the adsorption of sulfamethoxazole, carbamazepine and trimethoprim in the ternary system (in relation to single adsorption) and by Jung et al. (2015), who observed a reduction of approximately 80% in binary systems and 95% in ternary systems when studying the competitive adsorption of naproxen, diclofenac and ibuprofen.

In summary, the experimental data of binary and ternary mixtures were adequately described by single component isotherm models, allowing for comparison of the adsorption parameters when in the presence of more than one adsorbate. The reduced individual maximum adsorption capacities obtained for the majority of the pharmaceuticals in the mixtures must be related with competitive effects.

3.3.2 Modelling of multi-component isotherms to binary mixtures data

One disadvantage of describing multi-component data with single component isotherms is the impossibility of directly determining competition/interaction coefficients between the adsorbates, when such competition occurs. Aiming the determination of competition parameters between adsorbates in binary solutions, fittings of experimental data to multi-component isotherm models were resolved. For this purpose, the competitive Langmuir model, non-competitive Langmuir model and partially competitive Langmuir model, according to the equations 6 to 8 described in section 2.3.2, were considered. The competitive-Langmuir model was the only which reasonably described the binary adsorption data (fitting parameters are presented in Table 4). Correlation coefficients varied from 0.937 to 0.997 and, overall (with the only exception of the adsorption CBZ in the presence of PAR onto PBFG4), the estimated maximum adsorption capacity is in good agreement both with the experimental data and with the values obtained by the single component model fitting to the binary data. Additionally, the estimated K_L values (represented as K_{Li} in Table 4 for the pharmaceutical under analysis) by the multi-component model are also very close to the ones determined by the single component

Langmuir isotherm for the binary data (exception made to CBZ in the presence of PAR, for PS800-150-HCl, and CBZ in the presence of OXZ, for PBFG4). However, for the competitor pharmaceutical, K_L values (represented as K_{Lj}) are in general very low (also with some negative meaningless values); also, for example, K_{Li} for the pair OXZ (+CBZ) should be approximately the same of K_{Lj} of the pair CBZ (+OXZ) and this is not verified for any of the cases.

Regarding the other multi-component Langmuir related models (non-competitive and partially competitive), high correlation coefficients were obtained for the large majority of the fittings (generally, above 0.98). Nevertheless, generally, the estimated maximum adsorption capacities showed large deviations from those obtained experimentally and modelled by the single component isotherm. Additionally, the confidence limits of the determined parameters are extremely wide, resulting in the lack of chemical/physical significance of such parameters and eliminating the possibility of comparison between different systems. From our point of view, presenting the standard errors or confidence limits associated with the modelled parameters is essential for a proper comparison between systems and to understand, even with correlation coefficients close to 1, if the values have some physical meaning. However, when trying to compare the here obtained results with literature research studies on multi-component adsorption of organic compounds, it has been verified that standard deviation of the fitted parameters or the corresponding confidence limits are usually not presented (Fagundes-Klen et al., 2007; Ghaedi and Mosallanejad, 2014; Janaki et al., 2012; Kumar et al., 2008; Mahmoodi et al., 2011), eliminating the possibility of taking valid conclusions. Regarding the present work, the high standard error and confidence limits obtained for the referred multi-component isotherm models may be related to the number of experimental points used to describe a three-dimensional surface (the number of different adsorbent/adsorbate ratios varied from 8 to 10 in the studied systems). Unfortunately, considering a significantly higher number of experimental points in this context (multi-component experiments) is extremely time-consuming, being the main obstacle in this type of studies. In fact, probably due to the referred difficulties, it is common in the literature to use single component model parameters in multi-component equation to allow a reduction of variables to be modelled in the determination of competition

coefficients. These analyses are based on the assumption that the maximum adsorption capacity determined for single component data by the Langmuir isotherm is the same for multi-component systems (as this models implies adsorption onto homogeneous surfaces with no interactions between adsorbed species), suggesting that the Langmuir affinity coefficient is the only parameter to be modified in the presence of mixtures (Janaki et al., 2012; Limousin et al., 2007). However, this approach might be questionable considering that the presence of other adsorbates often result in a significant variation in the adsorption parameters (as it is clearly demonstrated in the data presented in Table 4) and might be responsible to introduce some artificiality in the data analysis.

There are some works showing that single component isotherms models successfully describe multi-component data (Al-Degs et al., 2007; Fernandez et al., 2014; Jung et al., 2015; Mansouri et al., 2015; Nielsen and Bandosz, 2016) which analyze the differences in the adsorbents' performance by comparing the modelled parameters obtained with single and multi-component data. Kumar et al. (2008) discussed the adequacy of the single *versus* multi-component isotherm models for the description of multi-component data, with 10 different multi-component models, reaching the conclusion that, despite high correlation coefficients, all of the tested models failed to accurately predict differences in the affinity of the adsorbates towards the adsorbent in the mixtures. In line with those conclusions, the present study also verified that mono-component isotherms were able to describe multi-component systems, providing useful information concerning the adsorption capacities and affinities of single *versus* binary systems. In this sense, the simplicity of single-component isotherm models, in comparison with multi-component ones, is undoubtedly a sound advantage in the application of those models in multi-solute systems.

4. Conclusions

This manuscript describes the adsorption of three pharmaceuticals (CBZ, PAR and OXZ) onto a non-activated waste-based carbon (PS800-150-HCl) and an activated commercial

carbon (PBFG4) either in single or in multi-solute solutions. Results from kinetics and equilibrium batch adsorption studies are consistent with the following conclusions:

- The single adsorption equilibrium is quickly attained both onto PBFG4 and, especially, onto PS800-150-HCl (maximum equilibrium times were approximately 120 and 15 min, respectively). Fast kinetics are maintained in binary and ternary systems, mostly with no significant reductions in the adsorption rate constants in comparison with single systems.

- Equilibrium experimental data (single and multi-component) were satisfactorily described by a single-component Langmuir isotherm. Single maximum adsorption capacities displayed by PBFG4 (between 272 ± 10 and 493 ± 12 μmol g^{-1}) were larger but more different between pharmaceuticals than in the case of PS800-150-HCl (between 64 ± 2 and 74 ± 1 μmol g^{-1}); nevertheless, maximum adsorption capacities follow the order CBZ>OXZ>PAR both onto PBFG4 and PS800-150HCl.

- For both carbons, single maximum adsorption capacities of each pharmaceutical decreased in the multi-component systems, suggesting the existence of competition between these pharmaceuticals; however, the decrease in the individual maximum adsorption capacities between single and multi-components systems was not higher than 50% in any case.

- Cumulative maximum adsorption capacities for binary and ternary systems are consistently higher than the single maximum adsorption capacities, indicating an actual increase in the total amount of pharmaceuticals adsorbed by the carbons.

- Langmuir competitive isotherm model satisfactorily described maximum adsorption capacities of multi-component systems, failing in predicting the Langmuir affinity adsorption coefficients.

5. Acknowledgments

This work was funded by FEDER through COMPETE 2020 and by national funds through FCT (*Fundação para a Ciência e Tecnologia*) by the research project PTDC/AAG-TEC/1762/2014. Vânia Calisto thanks the L'Oréal Foundation, FCT and UNESCO for funding through the L'Oréal Honour Medal for Women in Science, 2014 edition. Vânia Calisto and

Catarina I. A. Ferreira also thank FCT for their postdoctoral (SFRH/BPD/78645/2011) and PhD grants (SFRH/BD/88965/2012), respectively. Thanks are also due for the financial support to CESAM (UID/AMB/50017/2013), to FCT/MEC through national funds, and the co-funding by the FEDER, within the PT2020 Partnership Agreement and Compete 2020. Marta Otero acknowledges financial support from the Spanish Ministry of Economy and Competitiveness (RYC-2010-05634). The authors thank the kind collaboration of Engº Pedro Sarmento and Engº António Mendes de Sousa from RAIZ - *Instituto de Investigação da Floresta e do Papel*.

6. References

Al-Degs, Y., Khraisheh, M.A.M., Allen, S.J., Ahmad, M.N., Walker, G.M., 2007. Competitive adsorption of reactive dyes from solution: Equilibrium isotherm studies in single and multisolute systems. Chem. Eng. J. 128, 163–167.

Alygizakis, N.A., Gago-Ferrero, P., Borova, V.L., Pavlidou, A., Hatzianestis, I., Thomaidis, N.S., 2016. Occurrence and spatial distribution of 158 pharmaceuticals, drugs of abuse and related metabolites in offshore seawater. Sci. Total Environ. 541, 1097–105.

Bahlmann, A., Brack, W., Schneider, R.J., Krauss, M., 2014. Carbamazepine and its metabolites in wastewater: Analytical pitfalls and occurrence in Germany and Portugal. Water Res. 57, 104–14.

Bhatnagar, A., Sillanpää, M., 2010. Utilization of agro-industrial and municipal waste materials as potential adsorbents for water treatment—A review. Chem. Eng. J. 157, 277–296.

Calisto, V., Bahlmann, A., Schneider, R.J., Esteves, V.I., 2011a. Application of an ELISA to the quantification of carbamazepine in ground, surface and wastewaters and validation with LC–MS/MS. Chemosphere 84, 1708–1715.

Calisto, V., Domingues, M.R.M., Erny, G.L., Esteves, V.I., 2011b. Direct photodegradation of carbamazepine followed by micellar electrokinetic chromatography and mass spectrometry. Water Res. 45, 1095–1104.

Calisto, V., Esteves, V.I., 2009. Psychiatric pharmaceuticals in the environment. Chemosphere 77, 1257–1274.

Calisto, V., Ferreira, C.I.A., Oliveira, J.A.B.P., Otero, M., Esteves, V.I., 2015. Adsorptive removal of pharmaceuticals from water by commercial and waste-based carbons. J. Environ. Manage. 152, 83–90.

Calisto, V., Ferreira, C.I.A., Santos, S.M., Gil, M.V., Otero, M., Esteves, V.I., 2014. Production of adsorbents by pyrolysis of paper mill sludge and application on the removal of citalopram from water. Bioresour. Technol. 166, 335–344.

Cardoso, O., Porcher, J.-M., Sanchez, W., 2014. Factory-discharged pharmaceuticals could be a relevant source of aquatic environment contamination: Review of evidence and need for knowledge. Chemosphere 115, 20–30.

Daughton, C.G., Ternes, T.A., 1999. Pharmaceuticals and personal care products in the environment: Agents of subtle change? Environ. Health Perspect. 107, 907–938.

European Comission, 2014. Towards a circular economy:A zero waste programme for Europe

European Parliament, 2013. Directive 2013/39/EU of the European Parliament and of the Council of 12 August 2013 amending Directives 2000/60/EC and 2008/105/EC as regards priority substances in the field of water policy. Off. J. Eur. Union.

Fagundes-Klen, M.R., Ferri, P., Martins, T.D., Tavares, C.R.G., Silva, E.A., 2007. Equilibrium study of the binary mixture of cadmium–zinc ions biosorption by the Sargassum filipendula species using adsorption isotherms models and neural network. Biochem. Eng. J. 34, 136–146.

Fernandez, M.E., Ledesma, B., Román, S., Bonelli, P.R., Cukierman, A.L., 2015. Development and characterization of activated hydrochars from orange peels as potential adsorbents for emerging organic contaminants. Bioresour. Technol. 183, 221–8.

Fernandez, M.E., Nunell, G.V., Bonelli, P.R., Cukierman, A.L., 2014. Activated carbon developed from orange peels: Batch and dynamic competitive adsorption of basic dyes. Ind. Crops Prod. 62, 437–445.

Ferreira, C.I.A., Calisto, V., Santos, S.M., Cuerda-Correa, E.M., Otero, M., Nadais, H., Esteves, V.I., 2015. Application of pyrolysed agricultural biowastes as adsorbents for fish anaesthetic (MS-222) removal from water. J. Anal. Appl. Pyrolysis 112, 313–324.

Freundlich, H., 1906. Über die Adsorption in Lösungen. Zeitschrift für Phys. Chemie 57, 385-47.

Ghaedi, M., Mosallanejad, N., 2014. Study of competitive adsorption of malachite green and sunset yellow dyes on cadmium hydroxide nanowires loaded on activated carbon. J. Ind. Eng. Chem. 20, 1085–1096.

Gupta, V.K., Saleh, T.A., 2013. Sorption of pollutants by porous carbon, carbon nanotubes and fullerene- An overview. Environ. Sci. Pollut. Res. 20, 2828–2843.

Ho, Y.., McKay, G., 1999. Pseudo-second order model for sorption processes. Process Biochem. 34, 451–465.

Ioannidou, O., Zabaniotou, A., 2007. Agricultural residues as precursors for activated carbon production—A review. Renew. Sustain. Energy Rev. 11, 1966–2005.

Janaki, V., Vijayaraghavan, K., Ramasamy, A.K., Lee, K.-J., Oh, B.-T., Kamala-Kannan, S., 2012. Competitive adsorption of Reactive Orange 16 and Reactive Brilliant Blue R on polyaniline/bacterial extracellular polysaccharides composite--a novel eco-friendly polymer. J. Hazard. Mater. 241-242, 110–7.

Jelic, A., Gros, M., Ginebreda, A., Cespedes-Sánchez, R., Ventura, F., Petrovic, M., Barcelo, D., 2011. Occurrence, partition and removal of pharmaceuticals in sewage water and sludge during wastewater treatment. Water Res. 45, 1165–1176.

Jung, C., Boateng, L.K., Flora, J.R.V., Oh, J., Braswell, M.C., Son, A., Yoon, Y., 2015. Competitive adsorption of selected non-steroidal anti-inflammatory drugs on activated biochars: Experimental and molecular modeling study. Chem. Eng. J. 264, 1–9.

Kumar, D., Singh, A., Gaur, J.P., 2008. Mono-component versus binary isotherm models for Cu(II) and Pb(II) sorption from binary metal solution by the green alga Pithophora oedogonia. Bioresour. Technol. 99, 8280–7.

Lagergren, S.Y., 1898. Zur Theorie der sogenannten Adsorption gelöster Stoffe. K. Sven. Vetenskapsakademiens 24(4), 1-3.

Langmuir, I., 1918. The Adsorption of Gases on Plane Surfaces of Glass, Mica and Platinum. J. Am. Chem. Soc. 40, 1361–1403.

Li, W.C., 2014. Occurrence, sources, and fate of pharmaceuticals in aquatic environment and

soil. Environ. Pollut. 187, 193–201.

Limousin, G., Gaudet, J.P., Charlet, L., Szenknect, S., Barthès, V., Krimissa, M., 2007. Sorption isotherms: A review on physical bases, modeling and measurement. Appl. Geochemistry 22, 249–275.

Loos, R., Locoro, G., Comero, S., Contini, S., Schwesig, D., Werres, F., Balsaa, P., Gans, O., Weiss, S., Blaha, L., Bolchi, M., Gawlik, B.M., 2010. Pan-European survey on the occurrence of selected polar organic persistent pollutants in ground water. Water Res. 44, 4115–4126.

Luo, Y., Guo, W., Ngo, H.H., Nghiem, L.D., Hai, F.I., Zhang, J., Liang, S., Wang, X.C., 2014. A review on the occurrence of micropollutants in the aquatic environment and their fate and removal during wastewater treatment. Sci. Total Environ. 473–474, 619–641.

Mahmoodi, N.M., Salehi, R., Arami, M., 2011. Binary system dye removal from colored textile wastewater using activated carbon: Kinetic and isotherm studies. Desalination 272, 187–195.

Mansouri, H., Carmona, R.J., Gomis-Berenguer, A., Souissi-Najar, S., Ouederni, A., Ania, C.O., 2015. Competitive adsorption of ibuprofen and amoxicillin mixtures from aqueous solution on activated carbons. J. Colloid Interface Sci. 449, 252–60.

Margot, J., Kienle, C., Magnet, A., Weil, M., Rossi, L., de Alencastro, L.F., Abegglen, C., Thonney, D., Chèvre, N., Schärer, M., Barry, D.A., 2013. Treatment of micropollutants in municipal wastewater: Ozone or powdered activated carbon? Sci. Total Environ. 461–462, 480–498.

Mohan, D., Sarswat, A., Ok, Y.S., Pittman Jr, C.U., 2014. Organic and inorganic contaminants removal from water with biochar, a renewable, low cost and sustainable adsorbent – A critical review. Bioresour. Technol. 160, 191–202.

Nam, S.-W., Choi, D.-J., Kim, S.-K., Her, N., Zoh, K.-D., 2014. Adsorption characteristics of selected hydrophilic and hydrophobic micropollutants in water using activated carbon. J. Hazard. Mater. 270, 144–152.

Nielsen, L., Bandosz, T.J., 2016. Analysis of the competitive adsorption of pharmaceuticals on waste derived materials. Chem. Eng. J. 287, 139–147.

Noroozi, B., Sorial, G.A., 2013. Applicable models for multi-component adsorption of dyes: A review. J. Environ. Sci. 25, 419–429.

OECD, 2015. Health at a Glance 2015: OECD Indicators, OECD Publishing. Paris.

Sotelo, J.L., Ovejero, G., Rodríguez, A., Álvarez, S., Galán, J., García, J., 2014. Competitive adsorption studies of caffeine and diclofenac aqueous solutions by activated carbon. Chem. Eng. J. 240, 443–453.

Yu, Z., Peldszus, S., Huck, P.M., 2009. Adsorption of Selected Pharmaceuticals and an Endocrine Disrupting Compound by Granular Activated Carbon. 1. Adsorption Capacity and Kinetics. Environ. Sci. Technol. 43, 1467–1473.

Figure 1a)

Click here to download high resolution image

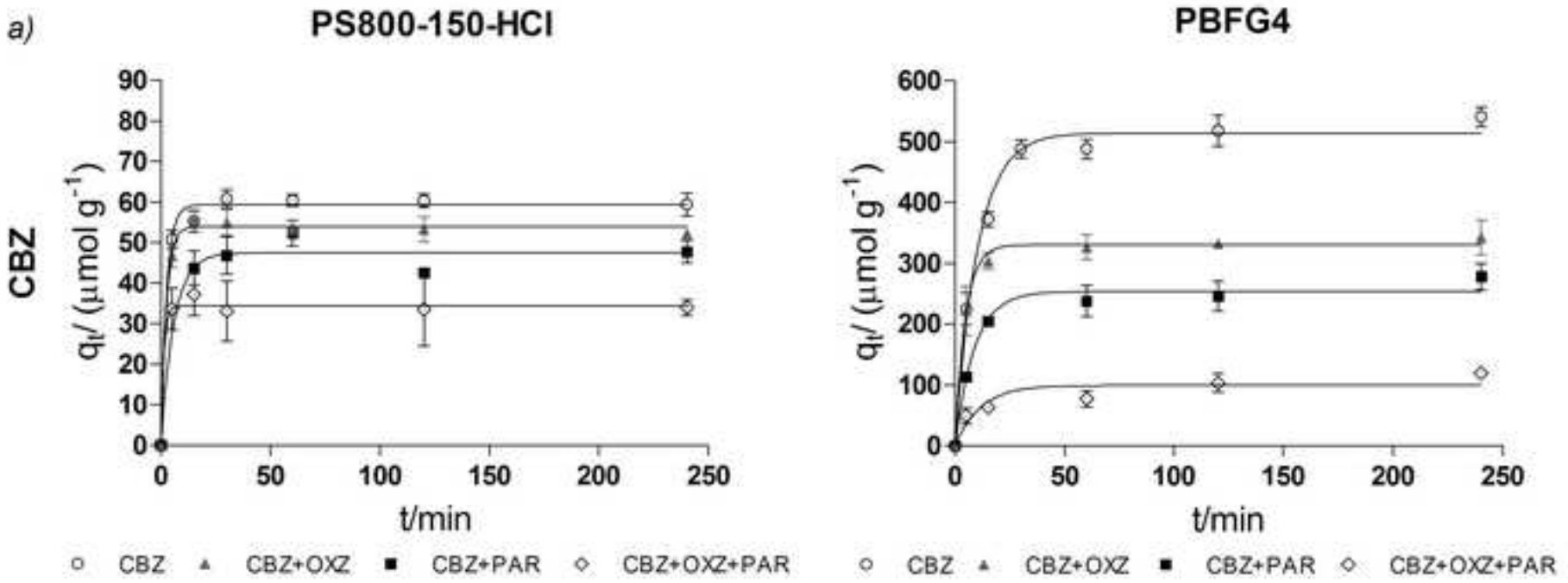

Figure 1a) color

Click here to download high resolution image

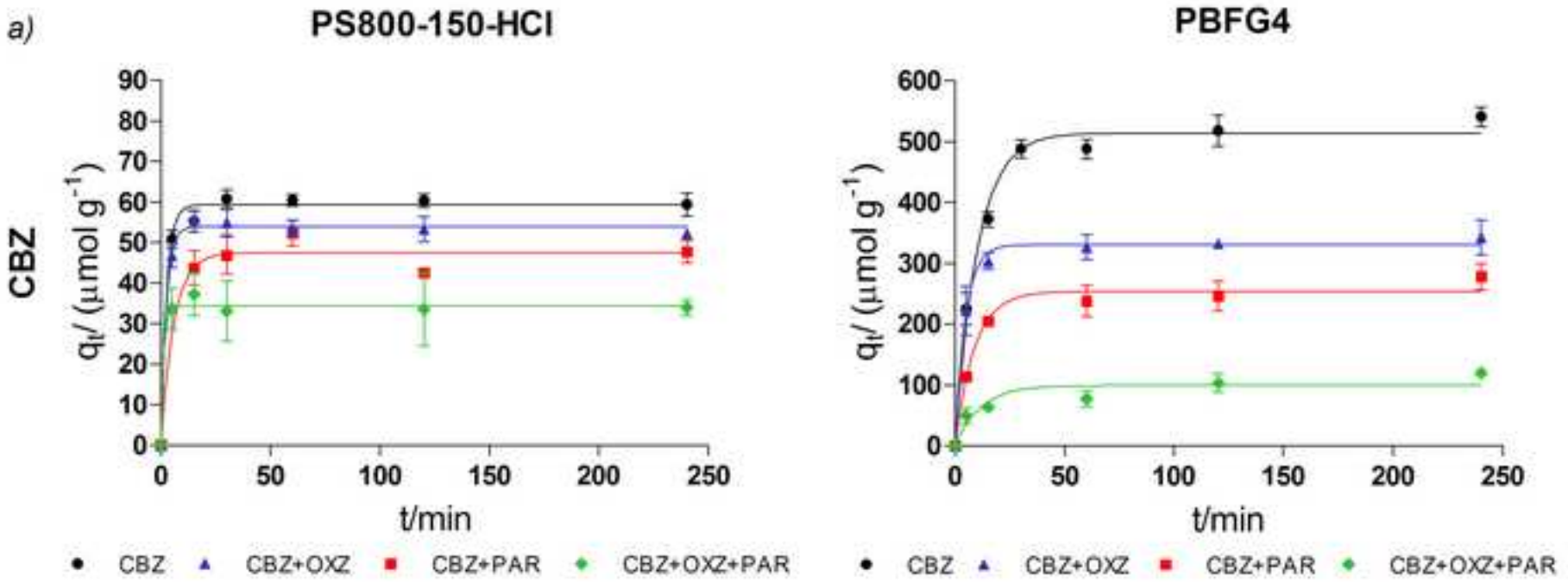

Figure 1b)

Click here to download high resolution image

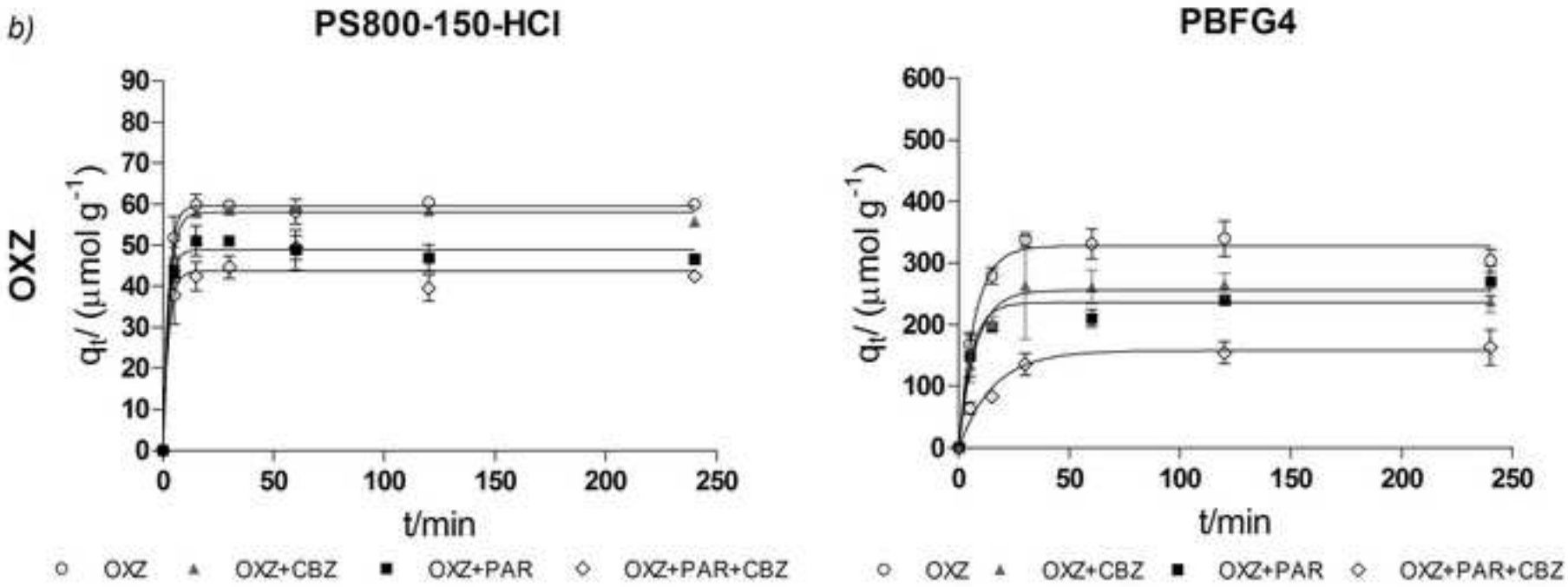

Figure 1b) color

Click here to download high resolution image

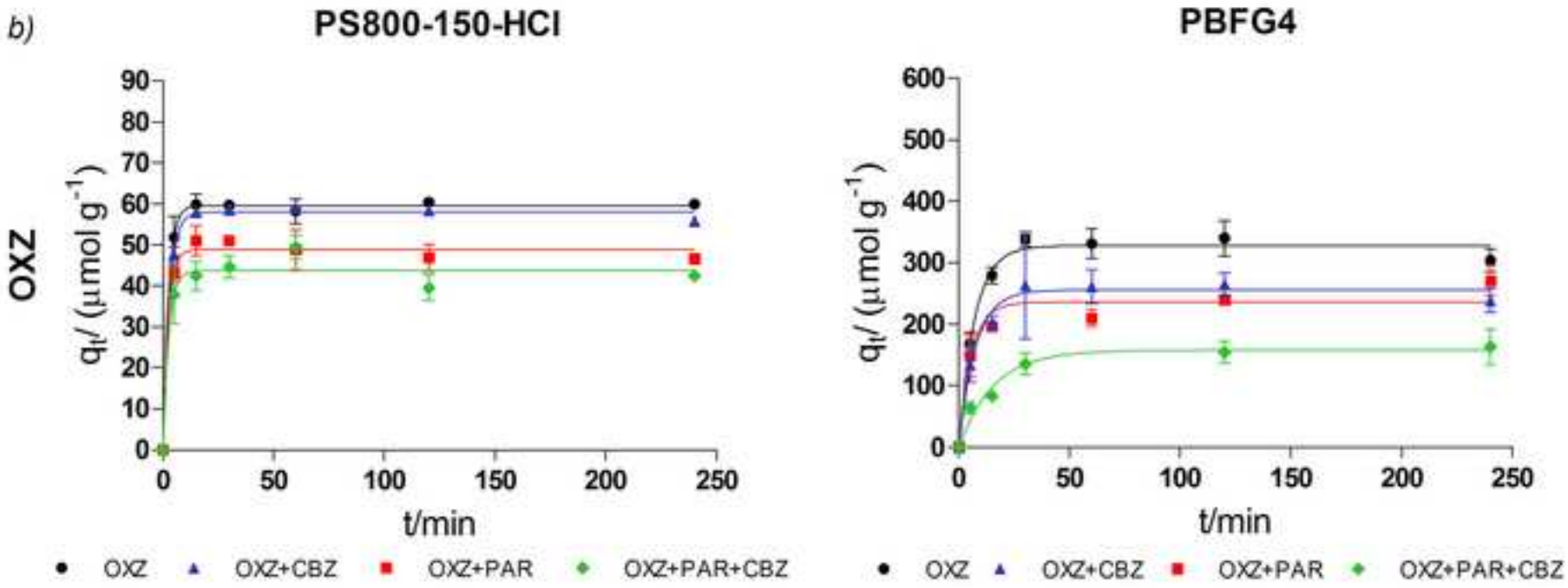

Figure 1c)

Click here to download high resolution image

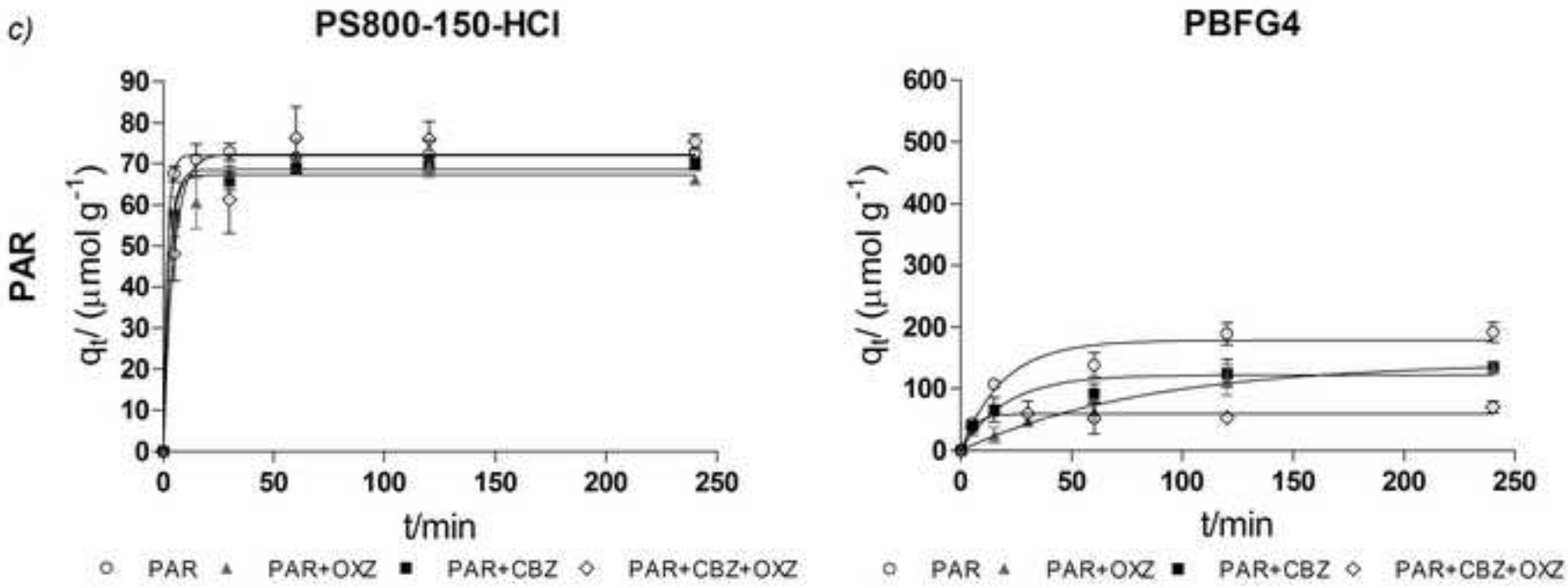

Figure 1c) color

Click here to download high resolution image

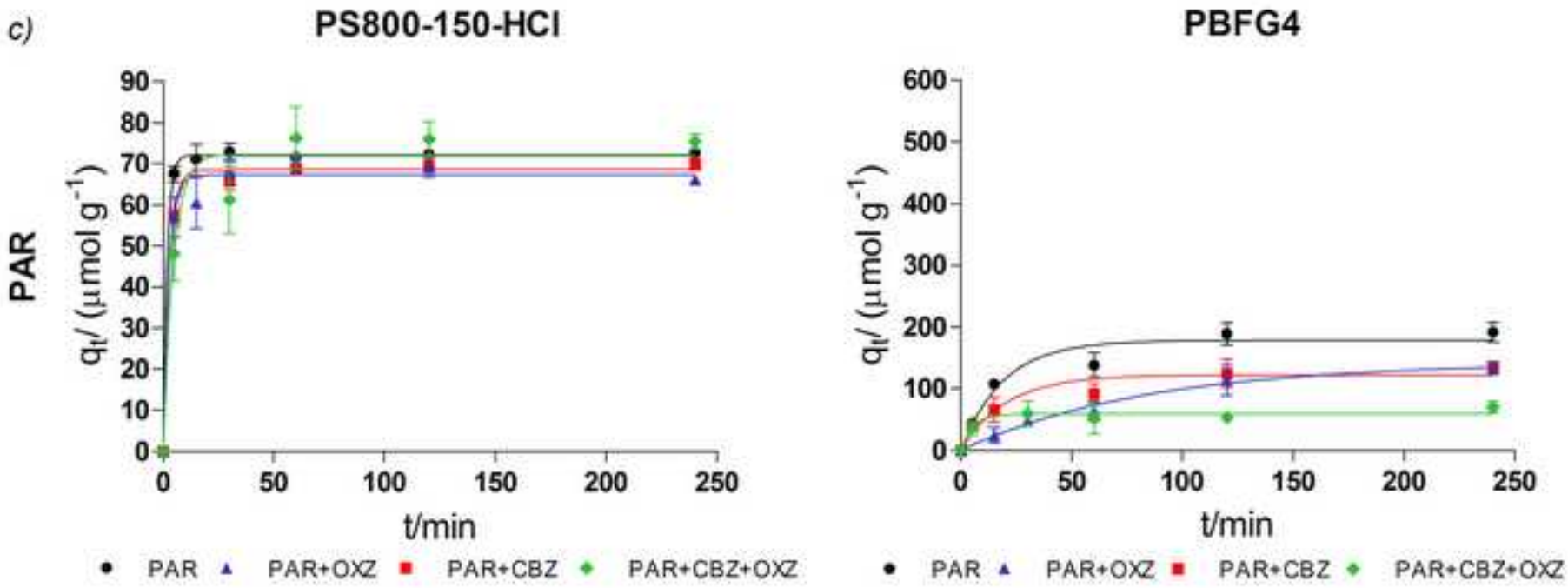

Figure 2

Click here to download high resolution image

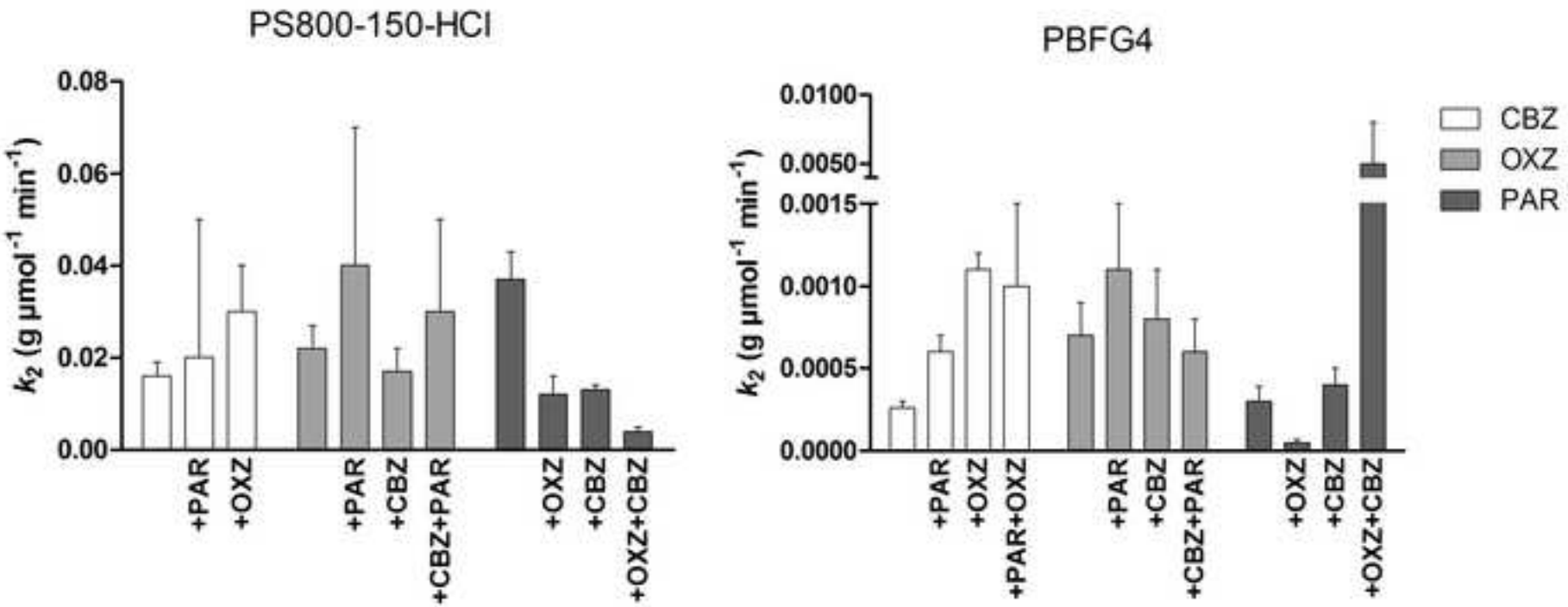

Figure 3a)

Click here to download high resolution image

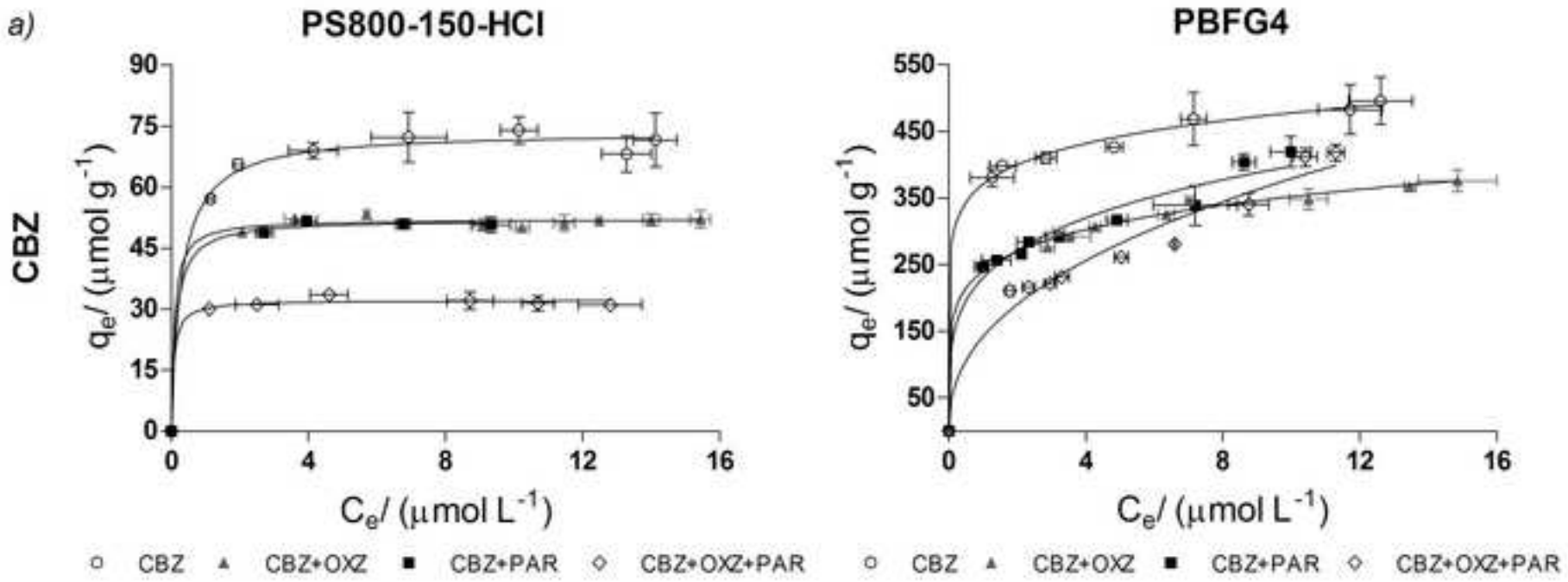

Figure 3a) color

Click here to download high resolution image

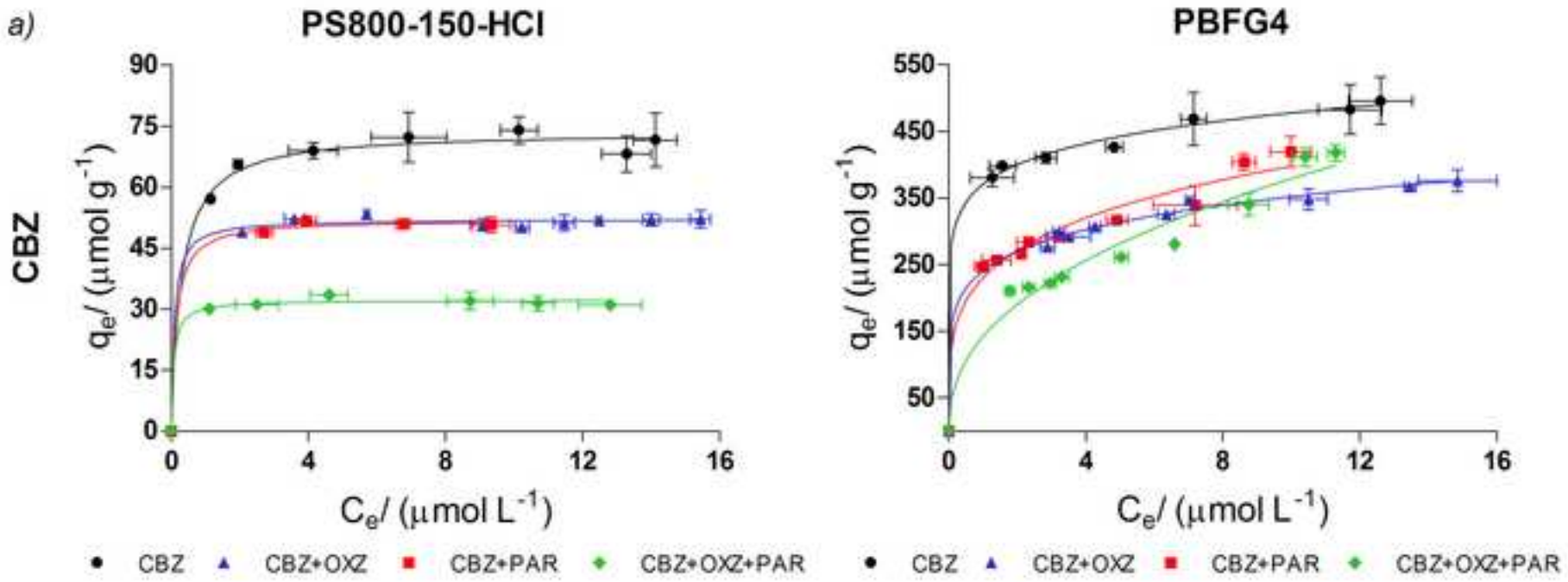

Figure 3b)

Click here to download high resolution image

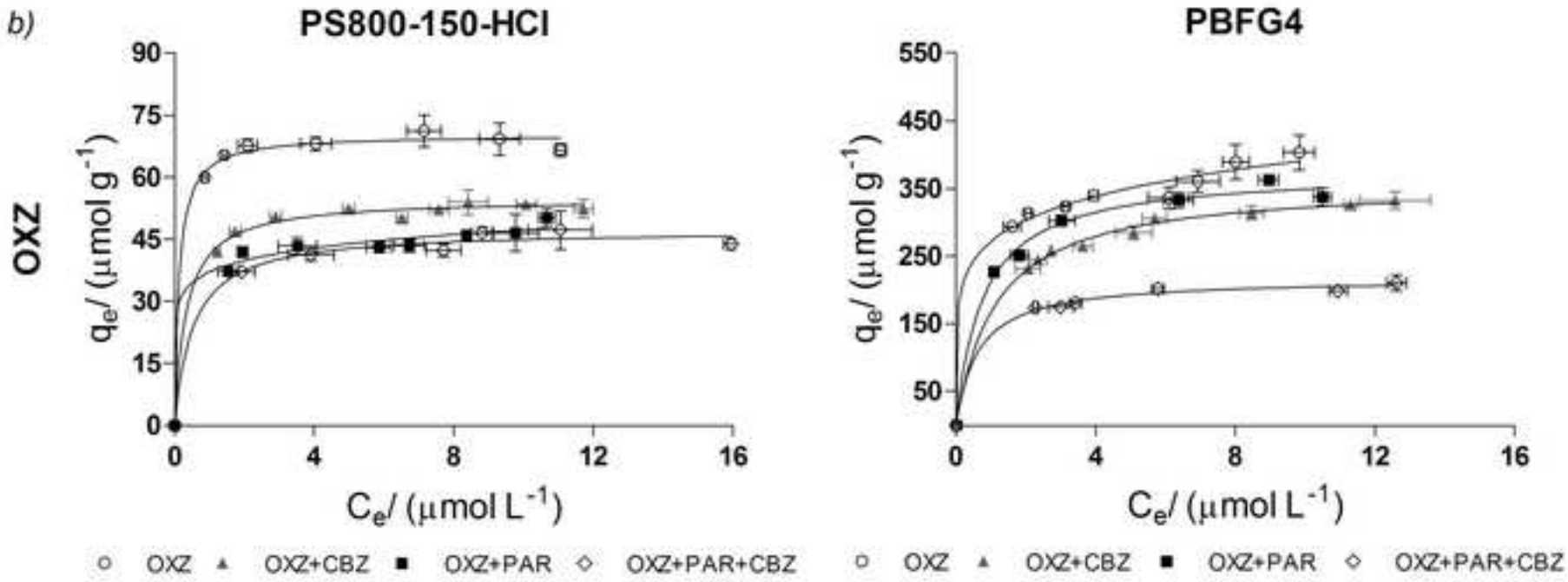

Figure 3b) color

Click here to download high resolution image

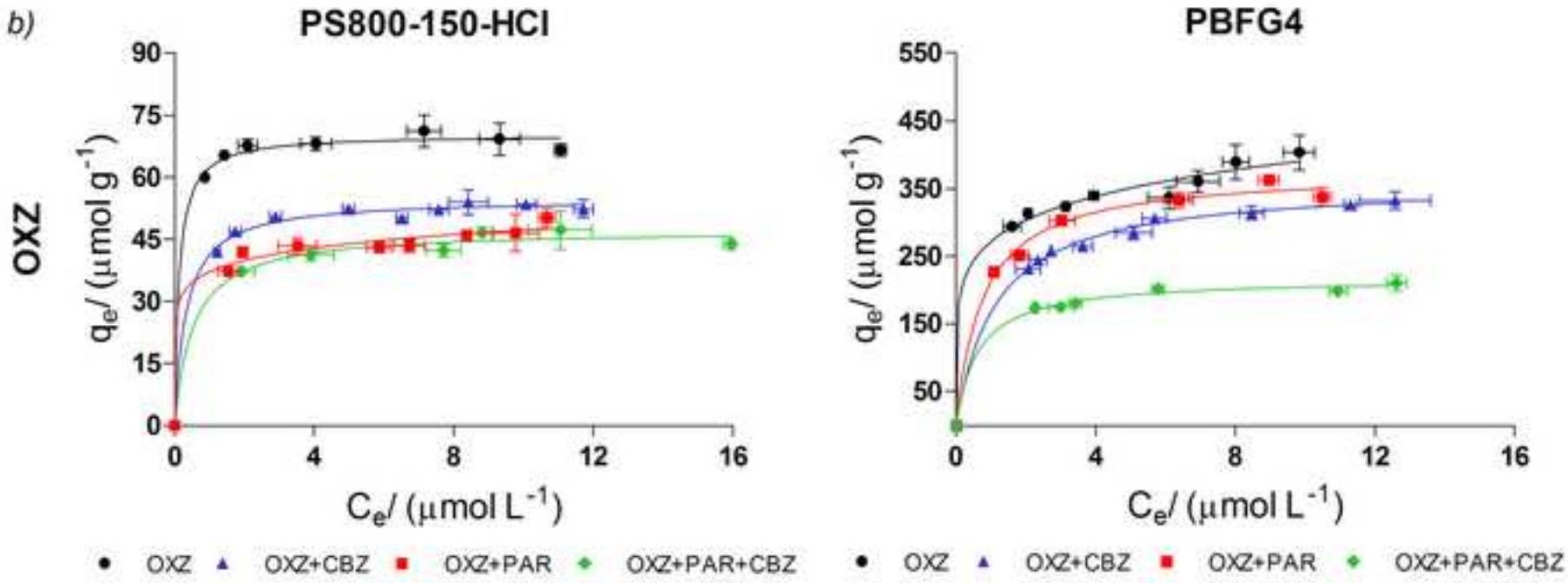

Figure 3c)

Click here to download high resolution image

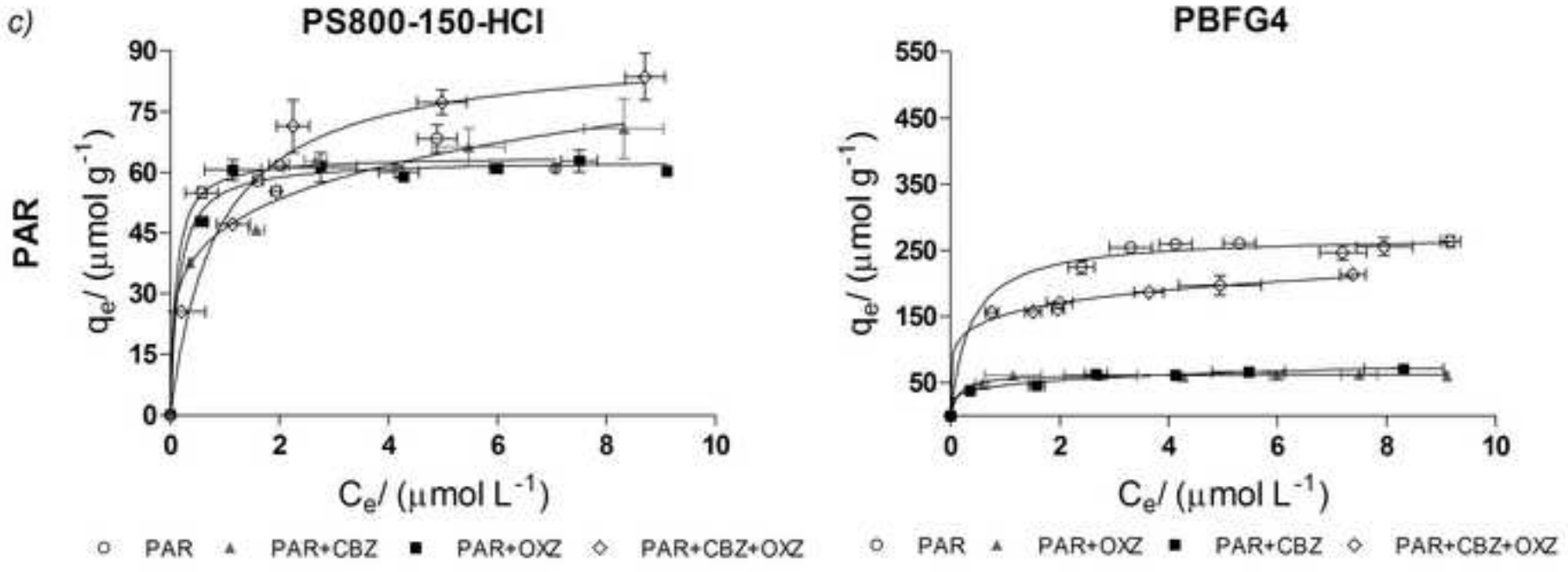

Figure 3c) color

Click here to download high resolution image

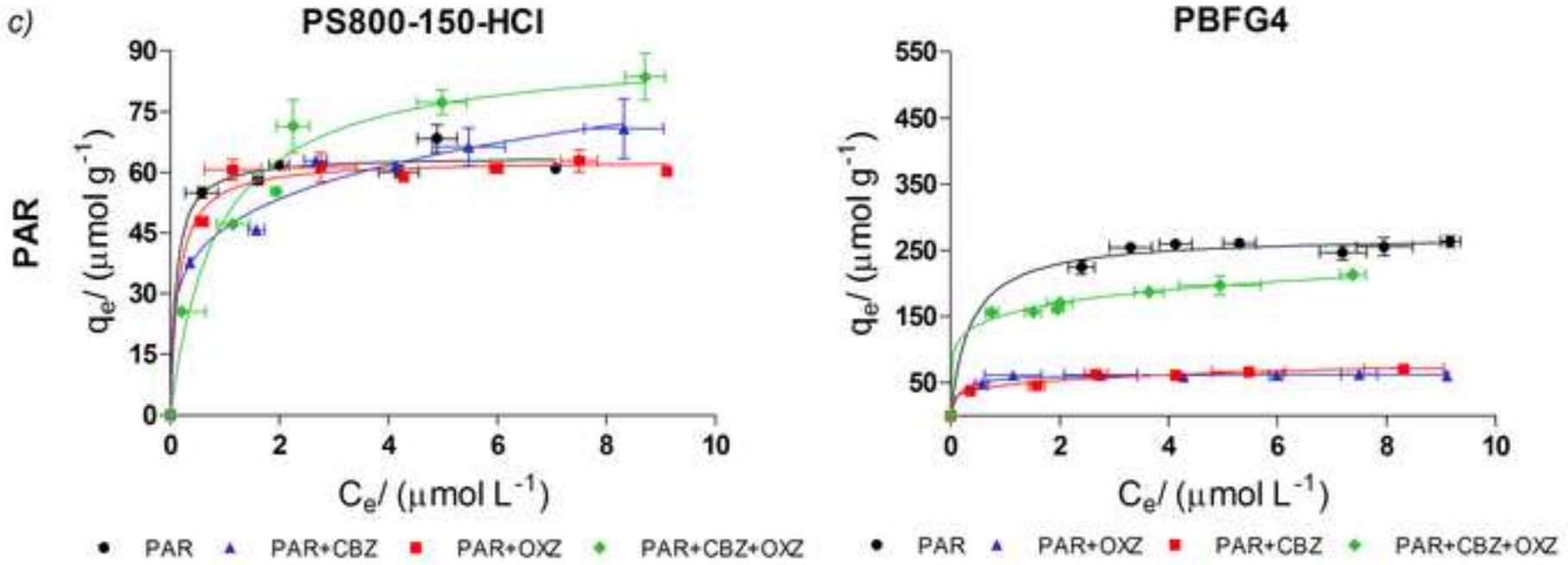

Figure 4

Click here to download high resolution image

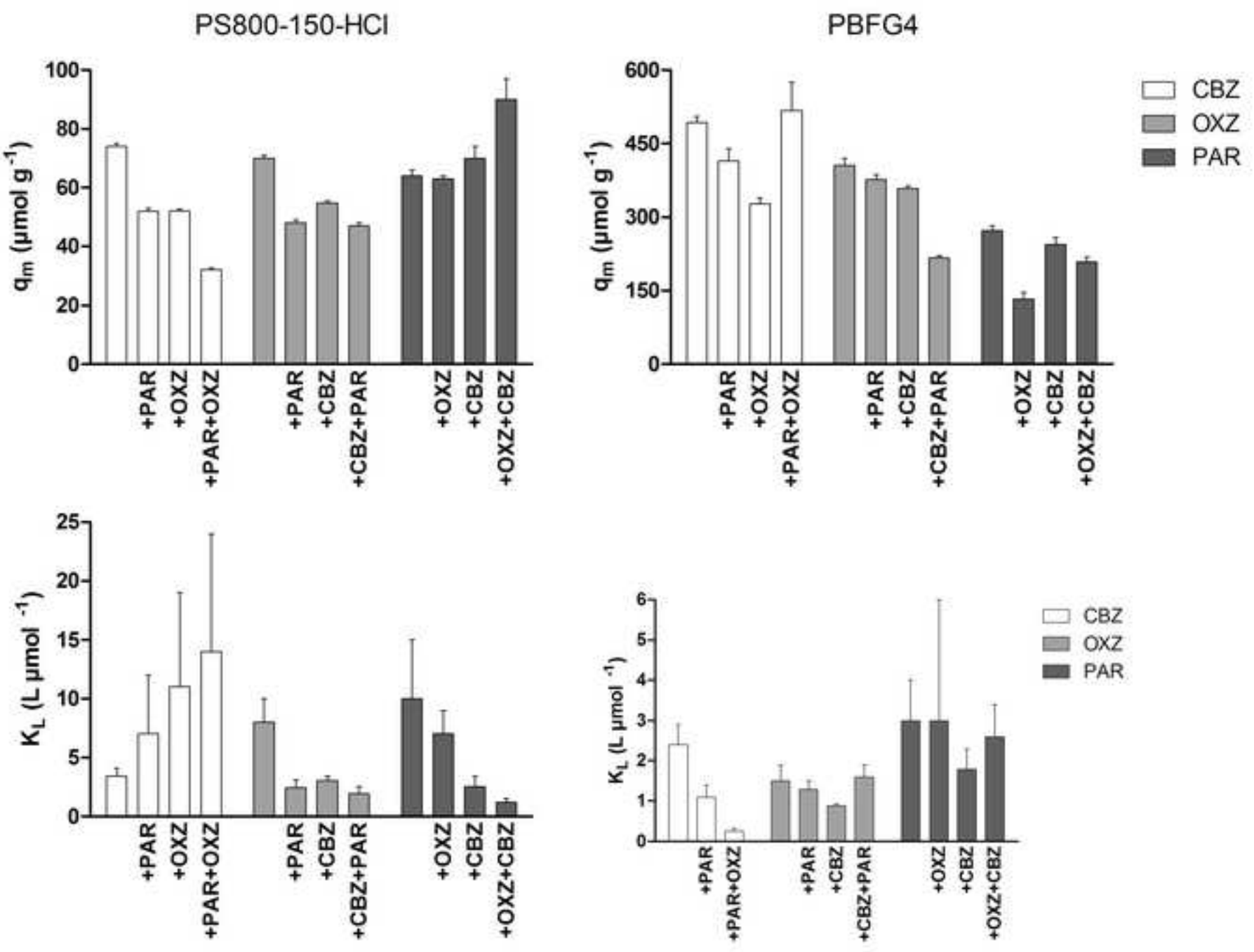

Figure 5

Click here to download high resolution image

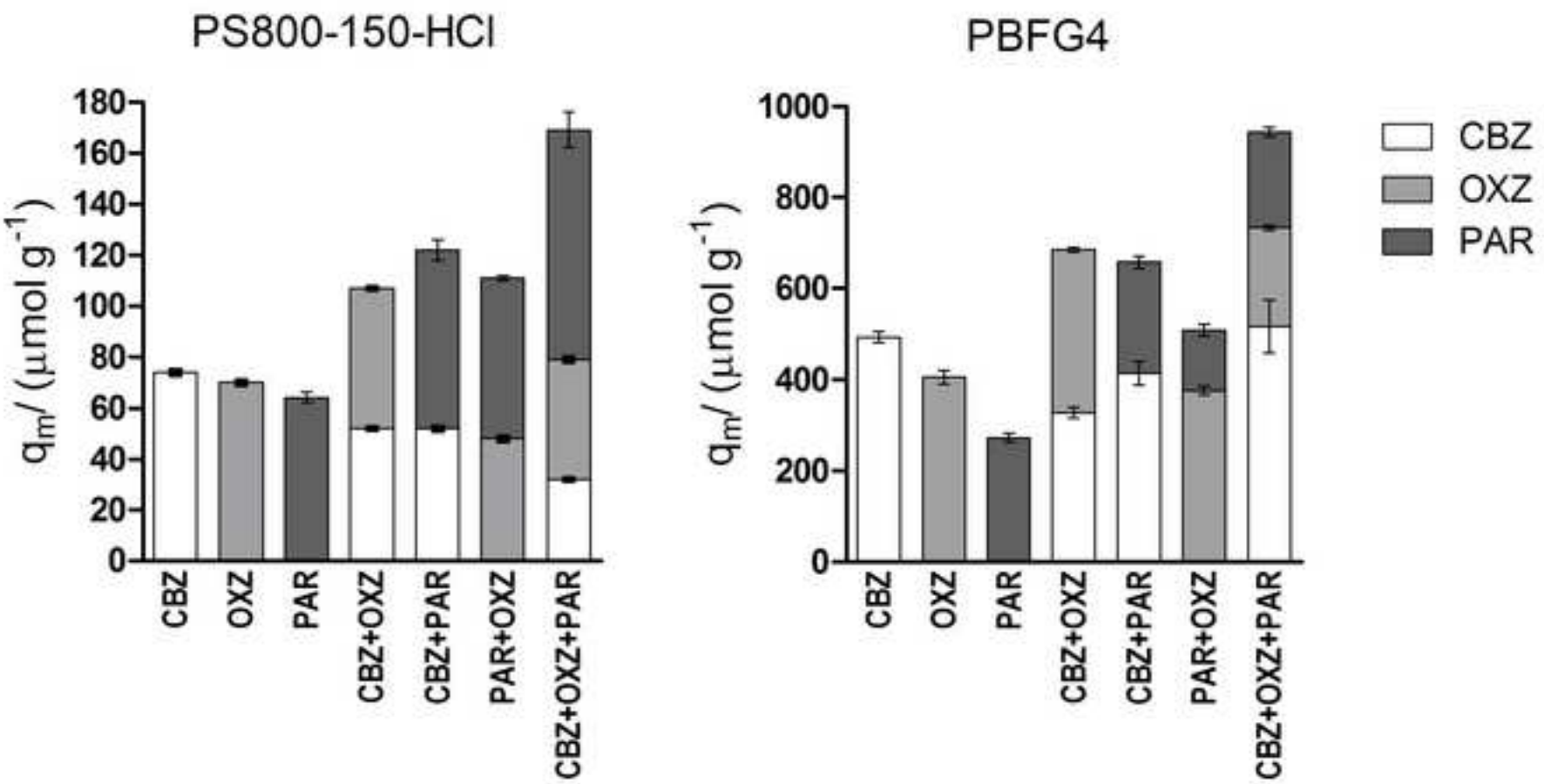

Figure 1 - Experimental and fitted data on the adsorption kinetics of *a)* CBZ, *b)* OXZ and *c)* PAR onto PS800-150-HCl and PBFG4 from single, binary and ternary systems. Each point represents the average of three replicates (± standard deviation). For clarity purposes, only fittings to the pseudo-second order model are shown (fitting parameters in Table 2).

Figure 2 – Pseudo-second order rate constants (k_2) from single, binary and ternary systems. Note that the y-axis scale is not the same in both graphs to allow a better visualization of the data.

Figure 3 - Experimental and fitted data on the adsorption equilibrium of *a)* CBZ, *b)* OXZ and *c)* PAR onto PS800-150-HCl and PBFG4 from single, binary and ternary systems. Each point represents the average of three replicates (± standard deviation). For clarity purposes, only fittings to the Langmuir isotherm model are shown (fitting parameters in Table 3).

Figure 4 – Maximum adsorption capacities (q_m) and Langmuir affinity constants (K_L) from single, binary and ternary systems. Note that the y-axis scale is not the same in all graphs to allow a better visualization of the data.

Figure 5 – Total maximum adsorption capacities of PS800-150-HCl and PBFG4 for single, binary and ternary systems. Note that the y-axis scale is not the same in both graphs to allow a better visualization of the data.

Table

Click here to download Table: Tables.docx

Table 1 – Elemental analysis (on a dry basis), total carbon analysis (total carbon (TC), inorganic carbon (IC) and organic carbon (OC)), N_2 adsorption isotherms (specific surface area (S_{BET}) and total micropore volume (W_0)) and Point of Zero Charge (PZC) of the primary sludge (raw material used for the production of PS800-150-HCl), PS800-150-HCl and PBFG4.

	Elemental Analysis (%)					**Total Carbon Analysis (%)**			**N_2 adsorption**		**PZC**
	C	*H*	*N*	*S*	*O*[1]	*TC*	*IC*	*OC*	S_{BET} /(m^2g^{-1})	W_0 /(cm^3g^{-1})	
Primary sludge[2]	14.8	1.26	0.40	0.29	27.9	33.0 ± 0.8	8.84 ± 0.05	24.1 ± 0.9	-	-	-
PS800-150-HCl	66.7	1.08	0.30	1.29	1.94	61.3 ± 0.5	0.01 ± 0.01	61.3 ± 0.5	414	0.095	7
PBFG4[3]	81.0	1.21	0.51	0.27	-	77.5 ± 0.1	0.04 ± 0.04	77.4 ± 0.2	848	0.36	6-7

[1] Estimated by difference: O (%) = 100 (%)-C-H-N-S-Ash
[2] Data from Calisto et al. (2014)
[3] Data from Jaria et al. (2015)

Table 2 – Fitting parameters of pseudo-first and pseudo-second order kinetic models to the experimental data[†]

		CBZ				OXZ				PAR			
		-	*+ PAR*	*+ OXZ*	*+PAR +OXZ*	-	*+ CBZ*	*+ PAR*	*+CBZ +PAR*	-	*+ CBZ*	*+ OXZ*	*+CBZ +OXZ*
PS800-150-HCl													
Pseudo-1st order	k_1	0.38 ± 0.05	0.17 ± 0.07	0.41 ± 0.04	0.8 ± 0.5	0.40 ± 0.02	0.35 ± 0.02	0.43 ± 0.08	0.4 ± 0.1	0.55 ± 0.03	0.36 ± 0.03	0.37 ± 0.08	0.22 ± 0.05
	q_e	59.3 ± 0.9	47 ± 2	54.0 ± 0.6	34.4 ± 0.8	59.6 ± 0.3	58.0 ± 0.5	48.8 ± 0.9	44 ± 1	72.1 ± 0.3	68.6 ± 0.9	67 ± 2	72 ± 3
	R^2	0.993	0.975	0.997	0.989	0.999	0.998	0.990	0.967	0.999	0.997	0.981	0.964
	S_{yx}	1.97	3.43	1.29	1.63	0.77	1.16	1.98	3.28	0.71	1.70	3.82	6.28
Pseudo-2nd order	k_2	0.016 ± 0.003	0.02 ± 0.03	0.03 ± 0.01	ambiguous	0.022 ± 0.005	0.017 ± 0.005	0.04 ± 0.03	0.03 ± 0.02	0.037 ± 0.006	0.013 ± 0.001	0.012 ± 0.004	0.004 ± 0.001
	q_e	60.8 ± 0.7	48 ± 3	55 ± 1	34.3 ± 0.7	60.6 ± 0.7	59 ± 1	49 ± 1	44 ± 2	72.8 ± 0.3	69.83 ± 0.01	69 ± 2	76 ± 3
	R^2	0.997	0.972	0.991	0.989	0.997	0.993	0.984	0.965	1.000	0.999	0.989	0.982
	S_{yx}	1.32	3.62	2.13	1.67	1.34	2.05	2.05	2.56	0.61	0.90	2.94	4.42
PBFG4													
Pseudo-1st order	k_1	0.10 ± 0.01	0.11 ± 0.02	0.21 ± 0.02	0.09 ± 0.04	0.14 ± 0.02	0.13 ± 0.02	0.18 ± 0.05	0.06 ± 0.01	0.05 ± 0.01	0.05 ± 0.02	0.12 ± 0.02	0.19 ± 0.07
	q_e	515 ± 12	254 ± 9	331 ± 5	100 ± 10	328 ± 7	256 ± 7	226 ± 14	158 ± 9	178 ± 12	122 ± 10	142 ± 8	59 ± 4
	R^2	0.989	0.984	0.996	0.867	0.989	0.983	0.945	0.965	0.952	0.929	0.989	0.933
	S_{yx}	22.64	15.05	9.61	17.29	14.16	13.88	25.21	13.09	19.07	15.49	5.92	7.18
Pseudo-2nd order	k_2	0.00026±0.00004	0.0006±0.0001	0.0011±0.0001	0.0010±0.0005	0.0007±0.0002	0.0008±0.0003	0.0011±0.0004	0.0006±0.0002	0.00030±0.00009	0.0004±0.0001	0.00005±0.00002	0.005±0.003
	q_e	558 ± 13	272 ± 9	344 ± 4	110 ± 10	346 ± 16	271 ± 12	250 ± 12	170 ± 9	203 ± 12	139 ± 9	191 ± 18	62 ± 4
	R^2	0.993	0.989	0.998	0.927	0.969	0.970	0.972	0.977	0.977	0.971	0.987	0.938
	S_{yx}	18.00	12.33	6.36	12.87	24.38	218.77	18.03	110.74	13.05	9.83	6.48	6.93

[†] k_1 (min^{-1}); k_2 (g μmol^{-1} min^{-1}); q_e (μmol g^{-1})

Table 3 – Fitting parameters of Freundlich and Langmuir models to the equilibrium experimental data[†]

		CBZ				OXZ				PAR			
		-	*+ PAR*	*+ OXZ*	*+PAR +OXZ*	-	*+ CBZ*	*+ PAR*	*+CBZ +PAR*	-	*+ CBZ*	*+ OXZ*	*+CBZ +OXZ*
PS800-150-HCl													
Freundlich	K_F	60 ± 2	49 ± 2	50 ± 1	30.8 ± 0.9	63 ± 2	44 ± 1	37 ± 1	36 ± 2	57 ± 2	46 ± 2	55 ± 2	48 ± 3
	N	14 ± 4	43 ± 41	78 ± 75	69 ± 79	25 ± 9	12 ± 2	9 ± 2	11 ± 3	18 ± 8	4.8 ± 0.7	16 ± 6	3.5 ± 0.5
	R^2	0.985	0.998	0.995	0.993	0.992	0.990	0.988	0.987	0.984	0.982	0.977	0.965
	S_{yx}	3.22	1.08	1.23	1.09	2.37	1.76	1.76	2.06	3.22	3.65	3.48	6.19
Langmuir	q_m	74 ± 1	52 ± 1	52.1 ± 0.6	32.2 ± 0.6	70 ± 1	54.8 ± 0.7	48 ± 1	47 ± 1	64 ± 2	70 ± 4	63 ± 1	90 ± 7
	K_L	3.4 ± 0.7	7 ± 5	11 ± 8	14 ± 10	8 ± 2	3.0 ± 0.4	2.4 ± 0.7	1.9 ± 0.6	10 ± 5	2.5 ± 0.9	7 ± 2	1.2 ± 0.3
	R^2	0.993	0.999	0.996	0.995	0.996	0.995	0.985	0.991	0.985	0.959	0.988	0.968
	S_{yx}	2.16	0.98	1.16	0.97	1.69	1.21	1.97	1.77	3.12	5.46	2.56	5.88
PBFG4													
Freundlich	K_F	371 ± 6	230 ± 10	240 ± 6	141 ± 13	272 ± 10	210 ± 5	232 ± 11	159 ± 5	226 ± 13	160 ± 6	113 ± 14	153 ± 4
	N	9.1 ± 0.7	4.2 ± 0.5	6.0 ± 0.5	2.3 ± 0.2	6.3 ± 0.9	5.4 ± 0.4	5.4 ± 0.7	9 ± 2	15 ± 8	5.1 ± 0.7	18 ± 27	6.3 ± 0.8
	R^2	0.998	0.977	0.996	0.967	0.990	0.995	0.988	0.995	0.989	0.984	0.946	0.992
	S_{yx}	8.52	18.47	7.63	22.95	12.61	6.93	15.02	5.66	10.42	10.37	13.23	6.35
Langmuir	q_m	493 ± 12	414 ± 26	327 ± 12	517 ± 58	405 ± 15	358 ± 5	376 ± 10	217 ± 5	272 ± 10	244 ± 14	133 ± 13	209 ± 10
	K_L	2.4 ± 0.5	1.1 ± 0.3	*ambiguous*	0.26 ± 0.07	1.5 ± 0.4	0.88 ± 0.06	1.3 ± 0.2	1.6 ± 0.3	3 ± 1	1.8 ± 0.5	3 ± 3	2.6 ± 0.8
	R^2	0.991	0.941	0.906	0.935	0.983	0.997	0.993	0.996	0.991	0.958	0.953	0.972
	S_{yx}	16.82	29.89	35.19	32.42	16.94	5.47	11.44	5.17	9.36	17.00	12.37	11.94

[†] K_F (μmol g^{-1} (μmol L^{-1})$^{-N}$); q_m (μmol g^{-1}); K_L (L μmol $^{-1}$)

Table 4 – Fitting parameters of the multi-component Langmuir competitive model to the binary systems equilibrium data[†]

	CBZ		**OXZ**		**PAR**	
	+ PAR	*+ OXZ*	*+ CBZ*	*+ PAR*	*+ CBZ*	*+ OXZ*
			PS800-150-HCl			
q_m	50 ± 20	57 ± 14	55 ± 2	50 ± 8	67 ± 35	60 ± 8
K_{Li}	> 10^5	7 ± 13	3 ± 1	1 ± 2	3 ± 4	4 ± 4
K_{Lj}	> 10^4	0.9 ± 2.1	<10^{-14}	<10^{-14}	0.0 ± 0.4	-0.1 ± 0.2
R^2	0.983	0.996	0.995	0.989	0.963	0.984
S_{yx}	2.798	1.121	1.205	1.988	5.461	2.650
			PBFG4			
q_m	610 ± 712	318 ± 135	358 ± 15	384 ± 81	212 ± 40	131 ± 36
K_{Li}	0.8 ± 1.0	1.1 ± 0.7	0.9 ± 0.2	1.3 ± 0.8	3 ± 4	5 ± 20
K_{Lj}	0.5 ± 1.3	-0.3 ± 0.6	<10^{-14}	0.0 ± 0.5	<10^{-10}	<10^{-14}
R^2	0.953	0.997	0.997	0.993	0.937	0.943
S_{yx}	28.53	6.84	5.47	12.62	17.74	12.63

[†] q_m (µmol g^{-1}); K_{Li} and K_{Lj} (L µmol $^{-1}$)

e-component

Click here to download e-component: Supplementary_material.docx